

Classifying pairs with trees for supervised biological network inference

Marie Schrynemackers¹ Louis Wehenkel¹ M. Madan Babu²

Pierre Geurts¹

¹Department of EE and CS & GIGA-R, University of Liège, Belgium

²MRC Laboratory of Molecular Biology, Cambridge, UK

September 28, 2018

Abstract

Networks are ubiquitous in biology and computational approaches have been largely investigated for their inference. In particular, supervised machine learning methods can be used to complete a partially known network by integrating various measurements. Two main supervised frameworks have been proposed: the local approach, which trains a separate model for each network node, and the global approach, which trains a single model over pairs of nodes. Here, we systematically investigate, theoretically and empirically, the exploitation of tree-based ensemble methods in the context of these two approaches for biological network inference. We first formalize the problem of network inference as classification of pairs, unifying in the process homogeneous and bipartite graphs and discussing two main sampling schemes. We then present the global and the local approaches, extending the later for the prediction of interactions between two unseen network nodes, and discuss their specializations to tree-based ensemble methods, highlighting their interpretability and drawing links with clustering techniques. Extensive computational experiments are carried out with these methods on various biological networks that clearly highlight that these methods are competitive with existing methods.

1 Introduction

In biology, relationships between biological entities (genes, proteins, transcription factors, micro-RNA, diseases, etc.) are often represented by graphs (or networks¹). In theory, most of these networks can be identified from lab experiments but in practice, because of the difficulties in setting up these experiments and their costs, we often have only a very partial knowledge of them. Because more and more experimental data become available about biological entities of interest, several researchers took an interest in using computational approaches to predict interactions between nodes in order to complete experimental predictions.

When formulated as a supervised learning problem, network inference consists in learning a classifier on pairs of nodes. Mainly two approaches have been investigated in the literature to adapt existing classification methods for this problem [38]. The first one, that we call the global approach, considers this problem as a standard classification problem on an input feature vector obtained by concatenating the feature vectors of each node from the pair [38]. The second approach, called local [2, 30], trains a different classifier for each node separately, aiming at predicting its direct neighbors in the graph. These two approaches have been mainly exploited with support vector machine (SVM) classifiers. In particular, several kernels have been proposed for comparing pairs of nodes in the global approach [1, 39]

¹In this paper, the terms network and graph will refer to the same thing.

and the global and local approaches can be related for specific choices of this kernel [23]. A number of papers applied the global approach with tree-based ensemble methods, mainly Random Forests [6], for the prediction of protein-protein [26, 9, 32, 36] and drug-protein [44] interactions, combining various feature sets. Besides the local and global methods, other approaches for supervised graph inference includes, among others, matrix completion methods [25], methods based on output kernel regression [19, 8], Random Forests-based similarity learning [31], and methods based on network properties [10].

In this paper, we would like to systematically investigate, theoretically and empirically, the exploitation of tree-based ensemble methods in the context of the local and global approaches for supervised biological network inference. We first formalize biological network inference as the problem of classification on pairs, considering in the same framework homogeneous graphs, defined on one kind of nodes, and bipartite graphs, linking nodes of two families. We then define the general local and global approaches in the context of this formalization, extending in the process the local approach for the prediction of interactions between two unseen network nodes. The paper discusses in details the specialization of these approaches to tree-based ensemble methods. In particular, we highlight their high potential in terms of interpretability and draw connections between these methods and unsupervised (bi-)clustering methods. Experiments on several biological networks show the good predictive performance of the resulting family of methods. Both the local and the global approaches are competitive with however an advantage for the local approach in terms of compactness of the inferred models.

The paper is structured as follows. Section 2 defines the general problem of classification on pairs and discusses two different sampling protocols in this context. Section 3 presents the global and local approaches and their particularization for tree ensembles. Section 4 relates experiments with these methods on several homogeneous and bipartite biological networks. Section 5 concludes and discusses future work directions. Additional results can be found in the appendix.

2 Network inference as classification on pairs

For the sake of generality, we assume that we have two finite sets of nodes, $U_r = \{n_r^1, \dots, n_r^{N_{U_r}}\}$ and $U_c = \{n_c^1, \dots, n_c^{N_{U_c}}\}$. An adjacency matrix Y of size $N_{U_r} \times N_{U_c}$ can then define a network connecting the two sets of nodes. An entry y_{ij} is equal to one if there is an edge between the nodes n_r^i and n_c^j , and zero if not. The subscripts r and c stand respectively for *row* and *column* of the adjacency matrix Y . Moreover, each node (or sometimes pair of nodes) is described by a feature representation given by $x(n)$ (or $x(n_r, n_c)$ for a pair), typically lying in \mathbb{R}^p . Y thus defines a partial *bipartite* graph over the two sets U_r and U_c . *Homogeneous* graphs defined on only one family of nodes can nevertheless be obtained as special cases of this general framework by considering only one universe of nodes ($U = U_r = U_c$). [33]

In this context, the problem of network inference can be cast as a problem of classification on pairs:

Given a partial knowledge of the adjacency matrix Y of the target network in the form of a learning sample of triplets:

$$LS_p = \{(n_r^i, n_c^j, y_{i,j}) | i = 1, \dots, N_{U_r}, j = 1, \dots, N_{U_c}\},$$

and given the feature representation of the nodes and/or pairs of nodes, find a function $f : U_r \times U_c \rightarrow \{0, 1\}$ that best approximates the unlabeled entries of the adjacency matrix from their feature representation (on nodes or on pairs).

Given a learning set LS_p of pairs labeled as interacting or not, the goal of a supervised network inference method is to get a prediction for the pairs not present in LS_p . All the pairs are not as easy as the others to predict: it is typically much more difficult to predict pairs with nodes for which no example of interactions are provided in the training network. One may thus partitioned the prediction into four families, depending on whether the nodes in the tested pair are represented or not in the learning set LS_p . Denoting by LS_c (resp. LS_r) the nodes from U_c (resp. U_r) that are present in LS_p (i.e. which are

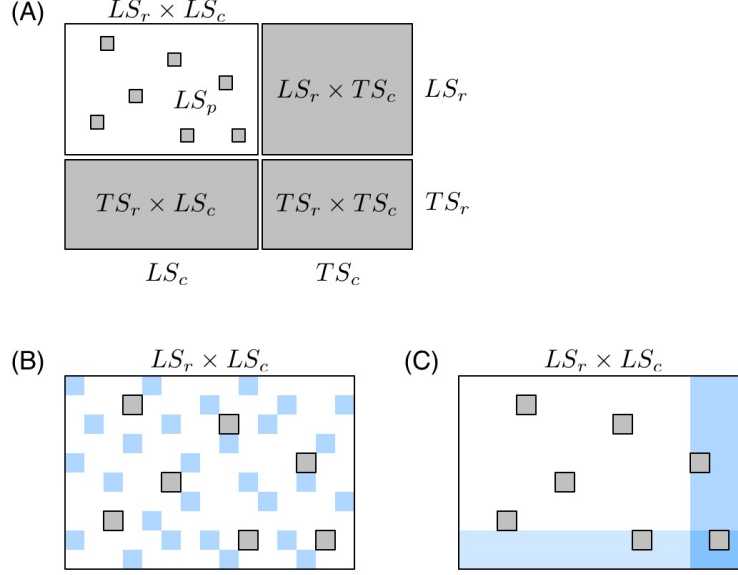


Figure 1: Schematic representation of known and unknown pairs in the network adjacency matrix (A) and of the two kinds of CV, CV on pairs (B) and CV on nodes (C). In (A): known pairs (that can be interacting or not) are in white and unknown pairs, to be predicted, are in gray. Rows and columns of the adjacency matrix have been rearranged to highlight the four families of unknown pairs described in the text: $LS_r \times LS_c$, $LS_r \times TS_c$, $TS_r \times LS_c$, and $TS_r \times TS_c$. In (B),(C): pairs from the learning fold are in white and pairs from the test fold are in blue. Pairs in gray represent unknown pairs that do not take part to the CV.

involved in some pairs in LS_p) and by $TS_c = U_c \setminus LS_c$ (resp. $TS_r = U_r \setminus LS_r$) unseen nodes from U_c (resp. U_r), the pairs of nodes to predict (i.e., outside LS_p) can be divided into the following four families:

- $(LS_r \times LS_c) \setminus LS_p$: predictions of (unseen) pairs between two nodes which are represented in the learning sample.
- $LS_r \times TS_c$ or $TS_r \times LS_c$: predictions of pairs between one node represented in the learning sample and one unseen node, where the unseen node can be either from U_c or from U_r .
- $TS_r \times TS_c$: predictions of pairs between two unseen nodes.

These families of pairs are represented in the adjacency matrix in Figure 1(A). Thereafter, we denote the four families as $LS \times LS$, $LS \times TS$, $TS \times LS$ and $TS \times TS$. In the case of an homogeneous undirected graph, only three sets can be defined as the two sets $LS \times TS$ and $TS \times LS$ are confounded. [33]

Prediction performance are expected to differ between these four families. Typically, one expects that $TS \times TS$ pairs will be the most difficult to predict since less information is available at training about the corresponding nodes. These predictions will then be evaluated separately in this work.

Cross-validation procedures evaluate supervised network inference methods. A first procedure (cross-validation on pairs) evaluates $LS \times LS$ pairs and is represented in Figure 1(B). A second one (cross-validation on nodes) evaluates $LS \times TS$, $TS \times LS$ and $TS \times TS$ pairs and is represented in Figure 1(C). [33]

3 Methods

In this section, we first present the two generic, local and global, approaches we have adopted for dealing with classification on pairs. We then discuss their practical implementation in the context of tree-based

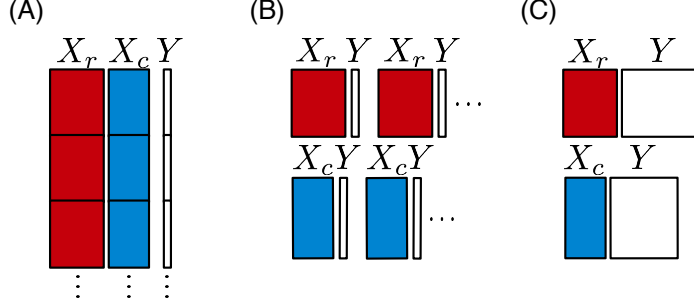


Figure 2: Schematic representation of the training data. In the global approach (A) the features vectors are concatenated, in the local approach with single output (B) one function is learnt for each node, and in the local approach with multiple output (C) one function is learnt for one family of nodes and one function for the other one.

ensemble methods. In the presentation of the approaches, we will assume that we have at our disposal a classification method that derives its classification model from a class conditional probability model. Denoting by $f : \mathcal{X} \rightarrow \{0, 1\}$ a classification model (defined on some input space \mathcal{X}), we will denote by $f^p : \mathcal{X} \rightarrow [0, 1]$ (i.e., with superscript p) the corresponding class conditional probability function (with $f(x) = 1(f^p(x) > p_{th})$ for some user-defined threshold $p_{th} \in [0, 1]$).

3.1 Global Approach

The most straightforward approach for dealing with the problem defined in Section 2 is to apply a classification algorithm on the learning sample LS_p of pairs to learn a function $f_{glob} : U_r \times U_c \rightarrow \{0, 1\}$ on the cartesian product of the two input spaces (resulting in the concatenation of the two input vectors of the nodes of the pair). Predictions can then be computed straightforwardly for any new unseen pair from the function. (Figure 2(A))

In the case of a homogeneous graph, the output function y is symmetric, i.e., $y(n_r, n_c) = y(n_c, n_r)$, $\forall n_r, n_c \in U$. We will introduce two adaptations of the approach to handle such graphs. First, for each pair (n_r, n_c) in the learning sample, the pair (n_c, n_r) will also be introduced in the learning sample. Without further constraint on the classification method, this will not ensure however that the learnt function f_{glob} will be symmetric in its arguments. To make it symmetric, we will compute a new class conditional probability model $f_{glob, sym}^p$ from the learned one f_{glob}^p as follows:

$$f_{glob, sym}^p(x_1, x_2) = \frac{f_{glob}^p(x_1, x_2) + f_{glob}^p(x_2, x_1)}{2}.$$

3.2 Local Approach

The idea of the local approach as first proposed in [2], is to build a separate classification model for each node, trying to predict its neighbors in the graph from the known graph around this node. More precisely, for every node $n_c \in LS_c$, a new learning sample $LS(n_c)$ is constructed from the learning sample of pairs LS_p as follows:

$$LS(n_c) = \{\langle n_r, y(n_r, n_c) \rangle \mid \langle n_r, n_c, y(n_r, n_c) \rangle \in LS_p\}.$$

It can then be used to learn a classification model $f_{n_c} : U_r \rightarrow \{0, 1\}$, which can be exploited to make a prediction for any new pair (n'_r, n'_c) such that $n'_c = n_c$. By symmetry, the same strategy can be adopted to learn a classification model $f_{n_r} : U_c \rightarrow \{0, 1\}$ for each node $n_r \in LS_r$. (Figure 2(B))

These two sets of classifiers can then be exploited to make $LS \times TS$ and $TS \times LS$ types of predictions. For pairs (n_r, n_c) in $LS_r \times LS_c \setminus LS_p$, two predictions can be obtained: $f_{n_c}(n_r)$ and $f_{n_r}(n_c)$. We propose

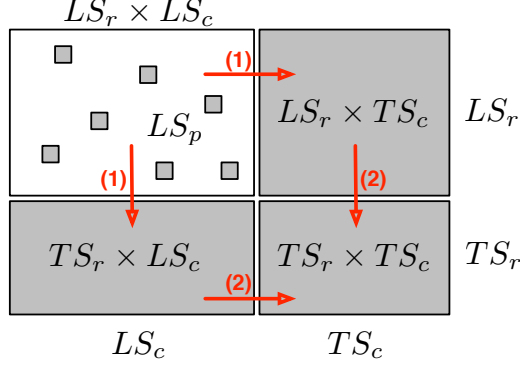


Figure 3: The local approach needs two steps to learn a classifier for an unseen node: first, we predict $LS \times TS$ and $TS \times LS$ interactions, and from these predictions, we predict $TS \times TS$ interactions.

to simply combine them by an arithmetic average of the corresponding class conditional probability estimates:

$$f_{loc}^p(n_r, n_c) = \frac{f_{n_c}^p(n_r) + f_{n_r}^p(n_c)}{2}.$$

As such, the local approach is in principle not able to make directly predictions for pairs of nodes $(n_r, n_c) \in TS \times TS$ (because $LS(n_r) = LS(n_c) = \emptyset$ for $n_r \in TS_r$ and $n_c \in TS_c$). We nevertheless propose to use the following two-steps procedure to learn a classifier for a node $n_r \in TS_r$ (see Figure 3):

- First, learn all classifiers f_{n_c} for nodes $n_c \in LS_c$,
- Then, learn a classifier $f_{n_r}^f : U_c \rightarrow \{0, 1\}$ from $LS^f(n_r) = \{(n_c, f_{n_c}(n_r)) | n_c \in LS_c\}$, i.e., the predictions given by the models f_{n_c} trained in the first step.

Again by symmetry, the same strategy can be applied to obtain models $f_{n_c}^f$ for the nodes $n_c \in TS_c$. A prediction is then obtained for a pair (n_r, n_c) in $TS \times TS$ by averaging the class conditional probability predictions of both models $f_{n_r}^{f,p}$ and $f_{n_c}^{f,p}$:

$$f_{loc}^p(n_r, n_c) = \frac{f_{n_r}^{f,p}(n_c) + f_{n_c}^{f,p}(n_r)}{2}.$$

Besides averaging, we tried several alternative schemes to merge the two models (such as taking the min, max, or the product of their predictions) but they did not lead to any improvement. Note that building the learning samples $LS^f(n_r)$ and $LS^f(n_c)$ requires to choose a threshold on the class conditional probability estimates. In our experiments, we will set this threshold in such a way that the proportion of edges versus non edges in the predicted subnetworks in $LS \times TS$ and $TS \times LS$ is equal to the same proportion within the original learning sample of pairs.

This strategy can be specialized to the case of a homogeneous graph in a straightforward way. Only one class of classifiers $f_n : U \rightarrow \{0, 1\}$ and $f_n^f : U \rightarrow \{0, 1\}$ are trained for nodes in LS and in TS respectively (using the same two-step procedure as in the asymmetric case for the second). $LS \times LS$ and $TS \times TS$ predictions are still obtained by averaging two predictions, one for each node of the pair.

3.3 Tree-based ensemble methods

Any method could be used as a base classifier for the two approaches. In this paper, we propose to evaluate the use of tree-based ensemble methods in this context. We first briefly describe these methods and then discuss several aspects related to their use within the two generic approaches.

Description of the methods. A decision tree [5] represents an input-output model by a tree whose interior nodes are each labeled with a (typically binary) test based on one input feature and each terminal node is labeled with a value of the output. The predicted output for a new instance is determined as the output associated to the leaf reached by the instance when it is propagated through the tree starting at the root node. A tree is built from a learning sample of input-output pairs, by recursively identifying, at each node, the test that leads to a split of the nodes sample into two subsamples that are as pure as possible in terms of their output values.

Single decision trees typically suffer from high variance, which makes them not competitive in terms of accuracy. This problem is circumvented by using ensemble methods that generate several trees and then aggregate their predictions. In this paper, we exploit one particular ensemble method called extremely randomized trees (Extra-trees, [17]). This method grows each tree in the ensemble by selecting at each node the best among K randomly generated splits. In our experiments, we use the default setting of K , equal to the square root of the total number of candidate attributes.

One interesting features of tree-based methods (single and ensemble) is that they can be extended to predict a vectorial output instead of a single scalar output [4]. We will exploit this feature of the method in the context of the local approach below.

Global approach. The global approach consists in building a tree from the learning sample of all pairs. Each split of the resulting tree will be based on one of the input features coming from either one of the two input feature vectors, $x(n_r)$ or $x(n_c)$. The tree growing procedure can thus be interpreted as interleaving the construction of two trees: one on the row nodes and one on the column nodes. Each leaf of the resulting tree is thus associated with a rectangular submatrix of the graph adjacency matrix $Y(LS_r, LS_c)$ and the construction of the tree is such that the pairs in this submatrix should be, as far as possible, either all connected or all disconnected (see Figure 4 for an illustration).

Local approach. The use of tree ensembles in the context of the local approach is straightforward. We will nevertheless compare two variants. The first one builds a separate model for each row and column nodes as presented in Section 3. The second method exploits the ability of tree-based methods to deal with multiple outputs to build only two models, one for the row nodes and one for the column nodes (Figure 2(C)). Assuming that the learning sample has been generated by sampling two subsets of objets $LS_r = \{n_r^1, \dots, n_r^{N_r}\}$ and $LS_c = \{n_c^1, \dots, n_c^{N_c}\}$ and that the full adjacency matrix is observed between these two sets, these two models are built from the following learning samples:

$$\begin{aligned} LS(n_c) &= \{\langle n_r^i, (y(n_r^i, n_c^1), \dots, y(n_r^i, n_c^{N_c})) \rangle \mid i = 1, \dots, N_r\}, \\ LS(n_r) &= \{\langle n_c^j, (y(n_r^1, n_c^j), \dots, y(n_r^{N_r}, n_c^j)) \rangle \mid j = 1, \dots, N_c\}. \end{aligned}$$

The same multiple output approach can then be applied to build the two models required to make $TS \times TS$ predictions. This approach has the advantage of requiring only four tree ensemble models in total instead of $N_r^U + N_c^U$ models for the single output approach. It can however only be used when the complete submatrix is observed for pairs in $LS \times LS$, since tree-based ensemble method can not cope with missing output values.

Interpretability. One main advantage of tree-based methods is their interpretability, directly through the tree structure in the case of single tree models and through feature importance rankings in the case of ensembles [18]. Let us to compare both approaches along this criterion.

In the case of the global approach, as illustrated in Figure 4(A), the tree that is built partitions the adjacency matrix $Y(LS_r, LS_c)$ into rectangular regions. These regions are defined such that pairs in each region are either all connected or all disconnect. The region is furthermore characterized by a path in the tree (from the root to the leaf) corresponding to tests on the input features of both nodes of the pair. In the case of the local multiple output approach, one of the two trees partitions the rows and the

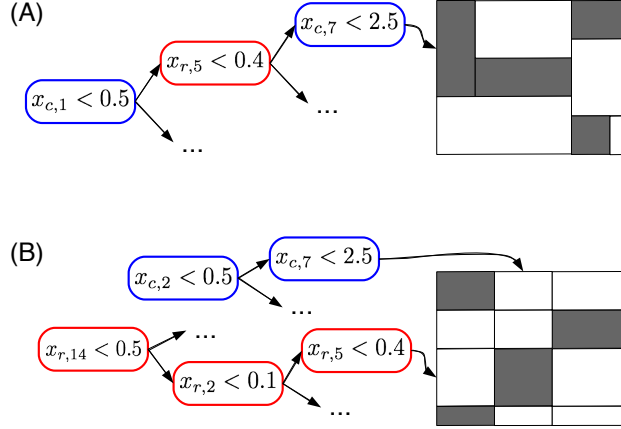


Figure 4: Both the global approach (A) and the local approach with multiple output (B) can be interpreted as carrying out a biclustering of the adjacency matrix. Note that in the case of the global approach, the representation is only illustrative. The adjacency submatrices corresponding to the tree leaves can not be necessarily rearranged as contiguous rectangular submatrices covering the initial adjacency matrix.

other tree partitions the column of the matrix $Y(LS_r, LS_c)$. Each partitioning is carried out in such a way that nodes in each subpartition has a similar connectivity profiles. The resulting partitioning of the adjacency matrix will thus follow a checkerboard structure with also only connected or disconnected pairs in the obtained submatrix, as far as possible (Figure 4(B)). Each submatrix will be furthermore characterized by two conjunctions of tests, one based on row inputs and one based on column inputs. These two methods can thus be interpreted as carrying out a biclustering [28] of the adjacency matrix where the biclustering is however directed by the choice of tests on the input features. These methods are to biclustering what predictive clustering trees [4] are to clustering. In the case of the local single output approach, the partitioning is more fine-grained as it can be different from one row or column to another. However in this case, each tree gives an interpretable characterization of the nodes which are connected to the node from which the tree was built.

When using ensembles, the global approach provides a global ranking of all features from the most to the less relevant. The local multiple output approach provides two separate rankings, one for the row features and one for the column features and the local single output approach gives a separate ranking for each node. All variants are therefore complementary from an interpretability point of view.

Implementation and computational issues. In principle, since tree building is a batch algorithm, the global approach requires to generate the full sample of all pairs, which may be very prohibitive for graphs defined on a large number of nodes (e.g., the PPI network used in our experiments contains about 1000 nodes that lead to about 1 millions pairs described by 650 attributes). Fortunately, since the tree building method goes through the input features one by one, one can separately search for the best split on features relative to nodes in U_r and on features relative to nodes in U_c , which does not require to generate explicitly the full data matrix. This is an important advantage with respect to kernel-based methods that typically requires to handle explicitly a $N_r N_c \times N_r N_c$ Gram matrix. Since tree growing is order $O(N \log(N))$ for a training sample of size N , the computational complexity of the whole procedure however remains $O(N_c N_r (\log(N_c) + \log(N_r)))$. The complexity of the trees (measured by the total number of nodes) is at worst $O(N_c N_r)$ (corresponding to a fully developed tree) but in practice it is related to the number of positive interactions in the training sample, which is typically much lower than $N_c N_r$.

The computational complexity of the local approach is the same as the computational complexity

Table 1: Summary of the six datasets used in the experiments.

| | Network | Network size | Number of edges | Number of features |
|-----------------------------|---------|--------------|-----------------|--------------------|
| <i>Homogeneous networks</i> | PPI | 984×984 | 2438 | 325 |
| | EMAP | 353×353 | 1995 | 418 |
| | MN | 668×668 | 2782 | 325 |
| <i>Bipartite networks</i> | ERN | 154×1164 | 3293 | 445/445 |
| | SRN | 113×1821 | 3663 | 9884/1685 |
| | DPI | 1862×1554 | 4809 | 660/876 |

of the global approach, i.e. $O(N_c N_r \log(N_r) + N_r N_c \log(N_c))$. Indeed, in the single output approach, N_c and N_r models need to be constructed respectively from N_r samples and N_c samples each. In the multiple output case, only two models are constructed from N_r and N_c samples respectively, but the multiple output variant needs to go through all outputs at each tree node, which multiplies complexity by respectively N_r and N_c for these two models. However, at worst, the complexity of the model is $O(N_c N_r)$ for the single output approach and $O(N_r + N_c)$ for the multiple output approach, which potentially gives an important advantage along this criterion for the multiple output method.

4 Experiments

In this section, we carried out a large scale empirical evaluation of the different methods described in Section 3 on six real biological networks, three homogeneous graphs and three bipartite graphs. Results on four additional (drug-protein) networks can be found in appendix A.2.3. Our goal with these experiments is to assess the relative performances of the different approaches and to give an idea of the performance one could expect from these methods on biological networks of different nature. Section 4.4 provides a comparison with existing methods from the literature.

4.1 Datasets

The first three networks correspond to homogeneous undirect graphs and the last three to bipartite graphs. The main characteristics of the datasets are summarized in Table 1.

Protein-protein interaction network (PPI). This network has been compiled from the 2438 high confidence interactions between 984 *S.cerevisiae* proteins highlighted by [29]. The input features used for the predictions are a set of expression data, phylogenetic profiles and localization data that totalizes 325 features. This dataset has been used in several studies before [41, 25, 19].

Genetic interaction network (EMAP). This network [34] contains 353 *S.cerevisiae* genes (nodes) connected with 1995 negative epistatic interactions (edges). Inputs consists in measures of growth fitness of yeast celln relative to deletion of each gene separately, and in 418 different environments. [21].

Metabolic network (MN). This network [42] is composed of 668 *S.cerevisiae* enzymes (nodes) connected by 2782 edges. There is an edge between two enzymes when these two enzymes catalyse successive reactions. The input feature vectors are the same as those used in the PPI network.

***E.coli* regulatory network (ERN).** This bipartite graph [15] connects transcription factors (TF) and genes of *E.coli*. It is composed of 1164 genes regulated by 154 TF. There is a total of 3293 interactions. The input features [15] are 445 expression values.

***S.cerevisiae* regulatory network (SRN).** This network [27] connects TFs and their target genes from *E.coli*. It is composed of 1855 genes regulated by 113 TFs and totalizing 3737 interactions. The input features are 1685 expression values [24, 22, 11, 16]. For genes, we concatenated motifs features [7] to the expression values.

Drug-protein interaction network (DPI). Drug-target interactions [40] are related to human and connect a drug with a protein when the drug targets the protein. This network holds 4809 interactions involving 1554 proteins and 1862 drugs. The input features are a binary vectors coding for the presence or absence of 660 chemical substructures for each drug, and the presence or absence of 876 PFAM domains for each protein [40].

4.2 Protocol

In our experiments, $LS \times LS$ performances in each network are measured by 10 fold cross-validation (CV) across the pairs of nodes, as illustrated in Figure 1(B). For robustness, results are averaged over 10 runs of 10 fold CV. $LS \times TS$, $TS \times LS$ and $TS \times TS$ predictions are assessed by performing a 10 times 10 fold CV across the nodes, as illustrated in Figure 1(C). The different algorithms return class conditional probability estimates. To assess our models independently of a particular choice of discretization threshold P_{th} on these estimates, we vary this threshold and output in each case the resulting precision-recall curve and the resulting ROC curve. Methods are then compared according to the total area under these curves, denoted AUPR and AUROC respectively (the higher the AUPR and the AUROC, the better), averaged over the 10 folds and the 10 CV runs. For all our experiments, we use ensembles of 100 extremely randomized trees with default parameter setting [17].

As highlighted by several studies, e.g. [20], in biological networks, nodes of high degree have a higher chance to be connected to any new node. In our context, this means that we can expect that the degree of a node will be a good predictor to infer new interactions involving this node. We want to assess the importance of this effect and provide a more realistic baseline than the usual random guess performance. To reach this goal, we evaluate the AUROC and AUPR scores when using the sum of the degrees of each node in a pair to rank $LS \times LS$ pairs and when using the degree of the nodes belonging to the LS to rank $TS \times LS$ or $LS \times TS$ pairs. AUROC and AUPR scores will be evaluated using the same protocol as hereabove. As there is no information about the degrees of nodes in $TS \times TS$ pairs, we will use random guessing as a baseline for the scores of these predictions (corresponding to an AUROC of 0.5 and an AUPR equal to the proportion of interactions among all nodes pairs).

4.3 Results

We discuss successively the results on the three homogeneous graphs and then on the three bipartite graphs.

Homogeneous graphs. AUPR and AUROC values are summarized in Table 2 for the three methods: global, local single output, and local multiple output. The last row on each dataset is the baseline result obtained as described in 4.2. Figure 5 shows the precision-recall curves obtained by the different approaches on MN, for the three different protocols. Similar curves for the two other networks can be found in appendix A.1.

In terms of absolute AUPR and AUROC values, $LS \times LS$ pairs are clearly the easiest to predict, followed by $LS \times TS$ pairs and $TS \times TS$ pairs. This ranking was expected from previous discussions. Baseline results in the case of $LS \times LS$ and $LS \times TS$ predictions confirm that nodes degrees are very informative: baseline AUROC values are much greater than 0.5 and baseline AUPR values are also significantly higher than the proportion of interactions among all pairs (0.005, 0.03, and 0.01 respectively for PPI, EMAP, and MN), especially in the case of $LS \times LS$ predictions. Nevertheless, our methods are

Table 2: Areas under curves for homogeneous networks.

| | | Precision-Recall (AUPR) | | | ROC (AUC) | | |
|-------------|----------|-------------------------|-------|-------|-----------|-------|-------|
| | | LS-LS | LS-TS | TS-TS | LS-LS | LS-TS | TS-TS |
| <i>PPI</i> | Global | 0.41 | 0.22 | 0.10 | 0.88 | 0.84 | 0.76 |
| | Local so | 0.28 | 0.21 | 0.11 | 0.85 | 0.82 | 0.73 |
| | Local mo | - | 0.22 | 0.11 | - | 0.83 | 0.72 |
| | Baseline | 0.13 | 0.02 | 0.00 | 0.73 | 0.74 | 0.50 |
| <i>EMAP</i> | Global | 0.49 | 0.36 | 0.23 | 0.90 | 0.85 | 0.78 |
| | Local so | 0.45 | 0.35 | 0.24 | 0.90 | 0.84 | 0.79 |
| | Local mo | - | 0.35 | 0.23 | - | 0.85 | 0.80 |
| | Baseline | 0.30 | 0.13 | 0.03 | 0.87 | 0.80 | 0.50 |
| <i>MN</i> | Global | 0.71 | 0.40 | 0.09 | 0.95 | 0.85 | 0.69 |
| | Local so | 0.57 | 0.38 | 0.09 | 0.92 | 0.83 | 0.68 |
| | Local mo | - | 0.45 | 0.14 | - | 0.85 | 0.71 |
| | Baseline | 0.05 | 0.04 | 0.01 | 0.75 | 0.70 | 0.50 |

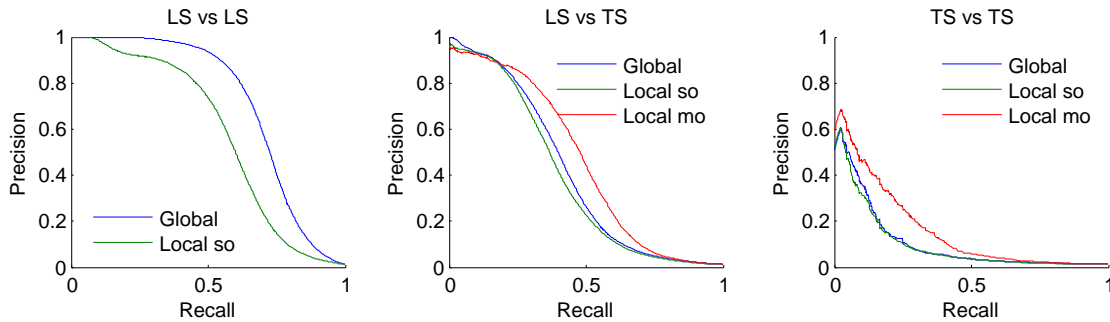


Figure 5: Precision-recall curves for metabolic network: higher is the number of nodes of a pair present in the learning set, better will be the prediction for this pair.

Table 3: Areas under curves for bipartite networks.

| | | Precision-Recall (AUPR) | | | | ROC (AUC) | | | |
|-----------------------------|----------|-------------------------|-------|-------|-------|-----------|-------|-------|-------|
| | | LS-LS | LS-TS | TS-LS | TS-TS | LS-LS | LS-TS | TS-LS | TS-TS |
| <i>ERN</i> (TF - gene) | Global | 0.78 | 0.76 | 0.12 | 0.08 | 0.97 | 0.97 | 0.61 | 0.64 |
| | Local so | 0.76 | 0.76 | 0.11 | 0.10 | 0.96 | 0.97 | 0.61 | 0.66 |
| | Local mo | - | 0.75 | 0.09 | 0.09 | - | 0.97 | 0.61 | 0.65 |
| | Baseline | 0.31 | 0.30 | 0.02 | 0.02 | 0.86 | 0.87 | 0.52 | 0.50 |
| <i>SRN</i> (TF - gene) | Global | 0.23 | 0.27 | 0.03 | 0.03 | 0.84 | 0.84 | 0.54 | 0.57 |
| | Local so | 0.20 | 0.25 | 0.02 | 0.03 | 0.80 | 0.83 | 0.53 | 0.57 |
| | Local mo | - | 0.24 | 0.02 | 0.03 | - | 0.83 | 0.53 | 0.57 |
| | Baseline | 0.06 | 0.06 | 0.03 | 0.02 | 0.79 | 0.78 | 0.51 | 0.50 |
| <i>DPI</i> (drug - protein) | Global | 0.14 | 0.05 | 0.11 | 0.01 | 0.76 | 0.71 | 0.76 | 0.67 |
| | Local so | 0.21 | 0.11 | 0.08 | 0.01 | 0.85 | 0.72 | 0.72 | 0.57 |
| | Local mo | - | 0.10 | 0.08 | 0.01 | - | 0.72 | 0.71 | 0.60 |
| | Baseline | 0.02 | 0.01 | 0.01 | 0.01 | 0.82 | 0.63 | 0.68 | 0.50 |

better than these baselines in all cases. On the EMAP network, the difference in terms of AUROC is very slight but the difference in terms of AUPR is important. This is typical of highly skewed classification problems, where precision-recall curves are known to give a more informative picture of the performance of an algorithm than ROC curves [12].

All tree-based approaches are very close on $LS \times TS$ and $TS \times TS$ pairs but the global approach has an advantage over the local one on $LS \times LS$ pairs. The difference is important on the PPI and MN networks. For the local approach, the performance of single and multiple output approaches are indistinguishable, except with the metabolic network where the multiple output approach gives better results. This is in line with the better performance of the global versus the local approach on this problem, as indeed both the global and the local multiple output approaches grow a single model that can potentially exploit correlations between the outputs. Notice that the multiple output approach is not feasible when we want to predict $LS \times LS$ pairs, as we are not able to deal with missing output values in multiple output decision trees.

Bipartite graphs. AUPR and AUROC values are summarized in Table 3 (see appendix A.2.3 for additional results on four DPI subnetworks). Figure 6 shows the precision-recall curves obtained by the different approaches on ERN for the four different protocols. Curves for the 6 other networks can be found in appendix A.2. 10 times 10-fold CV was used as explained in Section 4.2. Nevertheless, two difficulties appeared in the experiments performed on the DPI network. First, the dataset is larger than the others, and the 10-fold CV was replaced by 5-fold CV to reduce the computational space and time burden. Second, the feature vectors are binary and the randomization of the threshold (in Extra-Tree algorithm) cannot lead to diversity between the different trees of the ensemble. So we used bootstrapping to generate the training set of each tree.

Like for the homogeneous networks, higher is the number of nodes of a pair present in the learning set, better are the predictions, i.e., AUPR and AUROC values are significantly decreasing from $LS \times LS$ to $TS \times TS$ predictions. On the ERN and SRN networks, performances are very different for the two kinds of $LS \times TS$ predictions that can be defined, with much better results when generalizing over genes (i.e., when the TF of the pair is in the learning sample). On the other hand, on the DPI network, both kinds of $LS \times TS$ predictions are equally well predicted. These differences are probably due in part to the relative numbers of nodes of both kinds in the learning sample, as there are much more genes than TFs on ERN and SRN and a similar number of drugs and proteins in the DPI network. Differences are however probably also related to the intrinsic difficulty of generalizing over each node family, as on the four additional DPI networks (see appendix A.2.3), generalization over drugs is most of the time

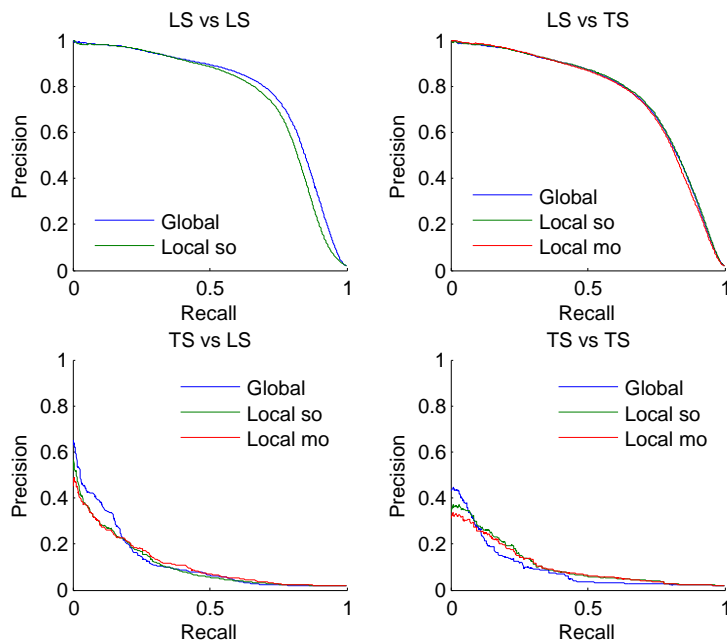


Figure 6: Precision-recall curves for E.coli regulatory network (TF vs genes): a prediction is easier to do if the TF belongs to the learning set than if the gene belongs to.

better than generalization over proteins, irrespectively of the relative numbers of drugs and proteins in the training network. Results are most of the time better than the baselines (based on nodes degrees for $LS \times LS$ and $LS \times TS$ predictions and on random guessing for $TS \times TS$ predictions). The only exceptions are observed when generalizing over TFs on SRN and when predicting $TS \times TS$ pairs on SRN and DPI.

The three approaches are very close to each other. Unlike on homonegeneous graphs, there is no strong difference between the global and the local approach on $LS \times LS$ predictions: it is slightly better in terms of AUPR on ERN and SRN but worse on DPI. The single and multiple output approaches are also very close, both in terms of AUPR and AUROC. Similar results are observed on the four additional DPI networks (appendix A.2.3).

4.4 Comparison with related works

In this section, we compare our methods with several other network inference methods from the literature. To ensure a fair comparison and avoid errors related to the reimplementaion and tuning of each of these methods, we choose to rerun our algorithms in similar settings as in related papers. All comparison results are summarized in Table 4 and discussed below.

Homogeneous graphs. [2] developed and applied the local approach with support vector machines to predict the PPI and MN networks and show that it was superior to several previous works [41, 25]. They only consider $LS \times TS$ predictions and used 5-fold CV. Although they exploited yeast-two-hybrid data as additional features for the prediction of the PPI network, we obtain very similar performances with the local multiple output approach (see Table 4). [19] use ensembles of output kernel trees to infer the MN and PPI networks with the same input data as [2]. With the global approach, we obtain similar or inferior results as [19] in terms of AUROC but much better results in terms of AUPR, especially on the MN data.

Bipartite graphs. [30] use SVM to predict ERN with the local approach, focusing on the prediction of interactions between known TFs and new genes ($LS \times TS$). They evaluated their performances by the

Table 4: Comparison with related works on the different networks.

| Publication | DB | Protocol | Measures | Their results | Our results |
|-------------|-----|---------------------------------|----------------|---------------|-------------|
| [2] | PPI | $LS \times TS$, 5CV | AUPR | 0.25 | 0.21 |
| | MN | | | 0.41 | 0.43 |
| [19] | PPI | $LS \times TS$, 10CV | AUPR / ROC | 0.18 / 0.91 | 0.22 / 0.84 |
| | | $TS \times TS$ | | 0.09 / 0.86 | 0.10 / 0.76 |
| | MN | $LS \times TS$ | | 0.18 / 0.85 | 0.45 / 0.85 |
| | | $TS \times TS$ | | 0.07 / 0.72 | 0.14 / 0.71 |
| [30] | ERN | $LS \times TS$, 3CV | Recall 60 / 80 | 0.44 / 0.18 | 0.38 / 0.15 |
| [40] | DPI | $LS \times LS$, 5CV | AUROC | 0.75 | 0.88 |
| [35] | DPI | $LS \times LS$, 5CV | AUROC | 0.87 | 0.88 |
| | | $LS \times TS$ & $TS \times LS$ | | 0.74 | 0.74 |

precision at 60% and 80% recall respectively, estimated by 3-fold CV (ensuring that all genes belonging to a same operon are always in the same fold). Our results with the same protocol (and the local multiple output variant) are very close although slightly less good. The DPI network was predicted in [40] using sparse canonical correspondence analyze (SCCA) and in [35] with the global approach and L_1 regularized linear classifiers using as input features all possible products of one drug feature and one protein feature. Only $LS \times LS$ predictions are considered in [40], while [35] differentiate “pair-wise CV” (our $LS \times LS$ predictions) and “block-wise CV” (our $LS \times TS$ and $TS \times LS$ predictions). As shown in Table 4, we obtain better results than [40] and similar results as in [35]. Additional comparisons are presented in appendix A.2.3 on the four DPI subnetworks.

Globally, these comparisons show that tree-based methods are competitive on all six networks. Moreover, it has to be noticed that (1) no other method has been tested over all these problems, and (2) we have not tuned any parameters of the Extra-trees method. Better performances could be achieved by changing, for example, the randomization scheme [6], the feature selection parameter K , or the number of trees.

5 Discussion

We explored tree-based ensemble methods for biological network inference, both with the local approach, which trains a separate model for each network node (single output) or each node family (multiple output), and with the global approach, which trains a single model over pairs of nodes. We carried out experiments on ten biological networks and compared our results with those from the literature. These experiments show that the resulting methods are competitive with the state of the art in terms of predictive performance. Other intrinsic advantages of tree-based approaches include their interpretability, through single tree structure and ensemble-derived feature importance scores, as well as their almost parameter free nature and their reasonable computational complexity and storage requirement.

While the local and global approaches are close in terms of accuracy, the most appealing approach in our experiments turns out to be the local multiple output method, which provides less complex models and requires less memory at training time. All approaches remain however interesting because of their complementarity in terms of interpretability. A potential advantage of the global approach that was not explored in this paper is the possibility to define features on pairs of nodes that might make a difference in some applications [26, 31, 35]. With the introduction of such features, one would loose however the possibility with tree-based methods of not generating explicitly all pairs when training the model.

As two side contributions, we extended the local approach for the prediction of edges between two

unseen nodes and proposed the use of multiple output models in this context. The two-step procedure used to obtain this kind of predictions provides similar results as the global approach, although it trains the second model on the first model’s predictions. It would be interesting to investigate other prediction schemes and evaluate this approach in combination with other supervised learning methods such as SVMs. The main benefits of using multiple output models is to reduce model sizes and potentially computing times, as well as to reduce variance, and therefore improving accuracy, by exploiting potential correlations between the outputs. It would be interesting to apply other multiple output or multi-label SL methods [37] within the local approach.

We focused on the evaluation and comparison of our methods on various biological networks. To the best of our knowledge, no other study has considered simultaneously as many of these networks. Our protocol defines an experimental testbed to evaluate new supervised network inference methods. Given our methodological focus, we have not tried to obtain the best possible predictions on each and every one of these networks. Obviously, better performances could be obtained in each case by using up-to-date training networks, by incorporating other feature sets, and by (cautiously) tuning the main parameters of tree-based ensemble methods. Such adaptation and tuning would not change however our main conclusions about relative comparisons between methods.

Our experiments, like others [35], show that the different families of predictions that are defined by the two protocols are not equally well predicted, which justifies their separate assessment. These discrepancies in terms of prediction quality should be taken into account when one wants to merge the different families of pairs into a single ranked list of novel candidate interactions from the more to the less confident as predicted by our models. This question largely deserves further study. A limitation of our protocol is that it assumes the presence of known positive and negative interactions. Most often in biological networks, only positive interactions are recorded, while all unlabeled interactions are not necessarily true negatives (a notable exception in our experiments is the EMAP dataset). In this work, we considered that all unlabeled examples are negative examples. It was shown empirically and theoretically that this approach is reasonable [14]. It would be interesting nevertheless to design tree-based ensemble methods that explicitly takes into account the absence of true negative examples (e.g., [13]).

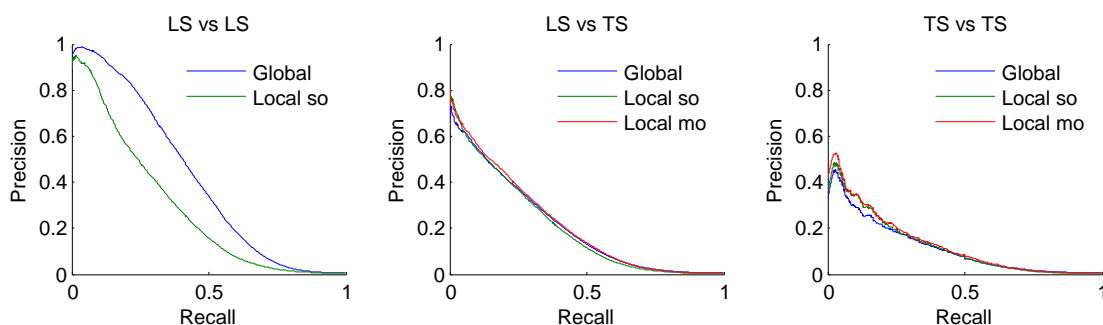
Acknowledgements

The authors thank the GIGA Bioinformatics platform and the SEGI for providing computing resources.

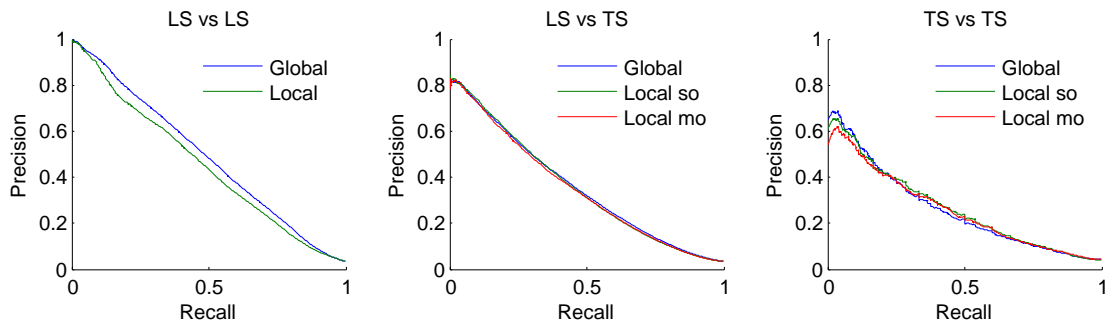
A Appendix

A.1 Homogeneous graphs

A.1.1 PPI network

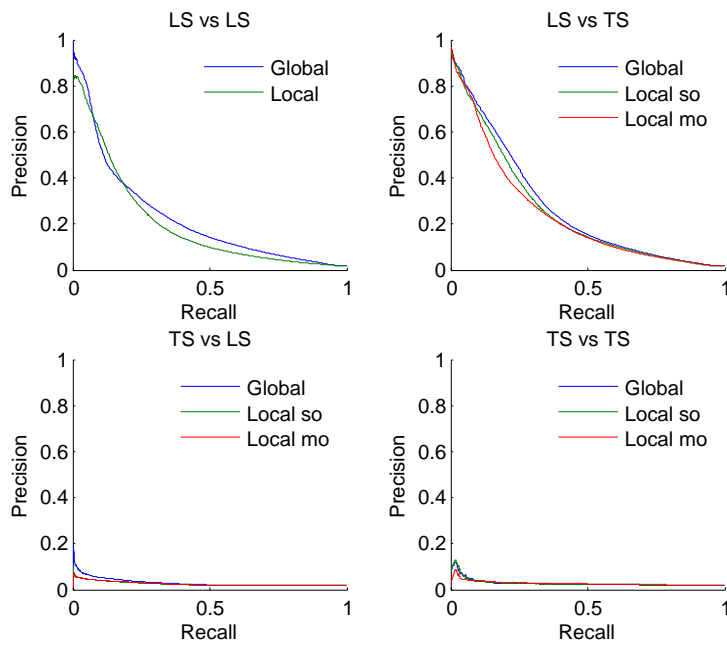


A.1.2 EMAP network

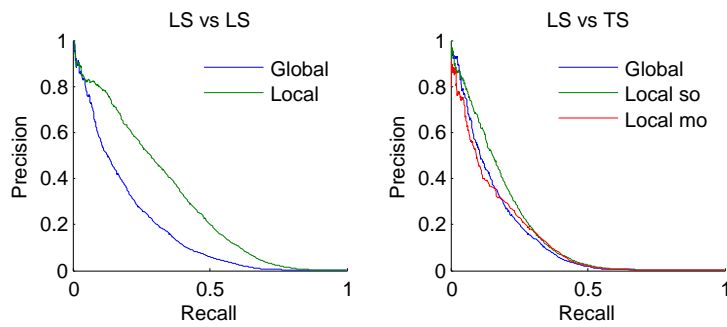


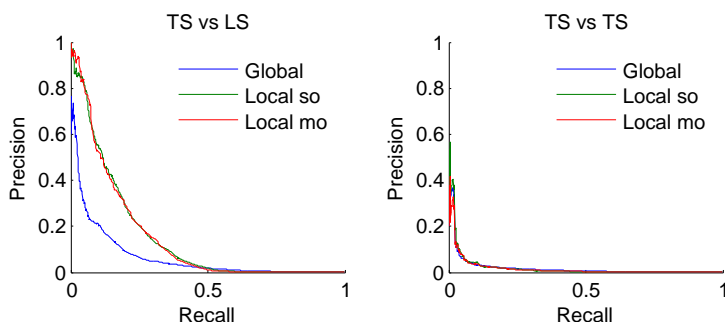
A.2 Bipartite graphs

A.2.1 *S.cerevisiae* regulatory network (TF vs genes)



A.2.2 Drug-protein interaction network





A.2.3 Four kinds of drug-protein interaction networks

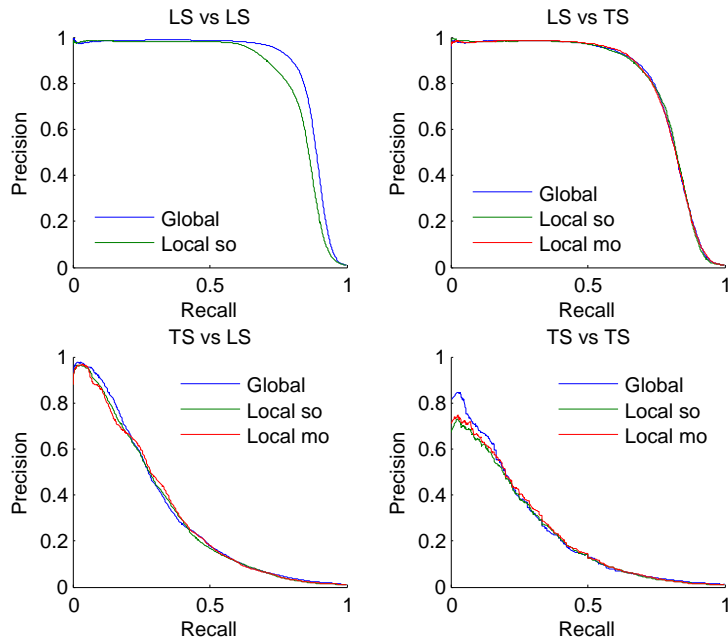
Datasets. [43] proposed four different drug-protein interaction networks in which proteins belong to four pharmaceutically useful classes: enzymes (DPI-E), ion channels (DPI-I), G-protein-coupled receptors (DPI-G) and nuclear receptors (DPI-N). The input features for proteins are similarity with all proteins in terms of sequence and the input features for drugs are similarity with all drugs in terms of chemical structure [43]. The number of drugs in these networks are respectively 445, 210, 223 and 54, the number of proteins are 664, 204, 95 and 26 and the number of interactions are 2926, 1476, 635 and 90.

| Network | Network size | # edges | # input features |
|---------|--------------|---------|------------------|
| DPI-E | 445×664 | 2926 | 445/664 |
| DPI-I | 210×204 | 1476 | 210/204 |
| DPI-G | 223×95 | 635 | 223/95 |
| DPI-N | 54×26 | 90 | 54/26 |

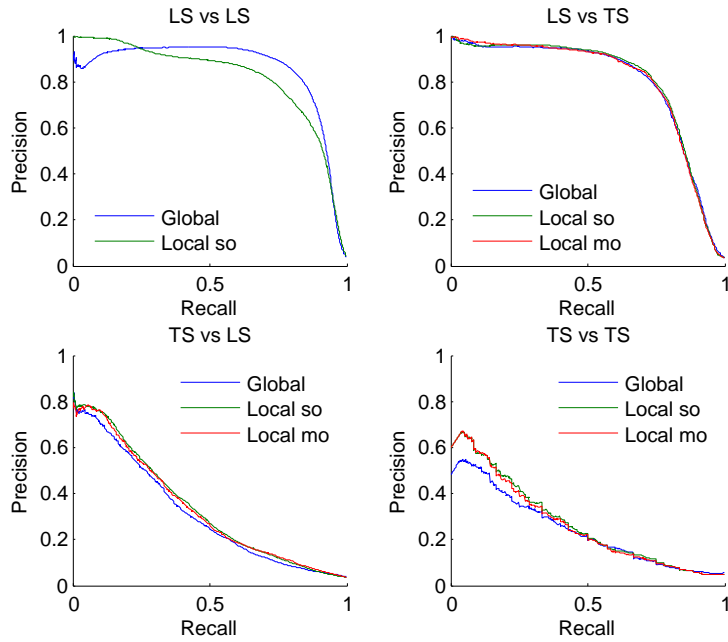
Results. Areas under precision-recall and ROC curves for the four networks:

| | Precision-Recall | | | | ROC | | | |
|-------------------------------------------------------------|------------------|-------|-------|-------|-------|-------|-------|-------|
| | LS-LS | LS-TS | TS-LS | TS-TS | LS-LS | LS-TS | TS-LS | TS-TS |
| <i>Drug-protein (enzyme) interaction network</i> | | | | | | | | |
| Global | 0.86 | 0.79 | 0.32 | 0.21 | 0.97 | 0.93 | 0.83 | 0.80 |
| Loc. so | 0.82 | 0.79 | 0.31 | 0.20 | 0.96 | 0.93 | 0.82 | 0.79 |
| Loc. mo | - | 0.79 | 0.32 | 0.21 | - | 0.93 | 0.82 | 0.78 |
| <i>Drug-protein (ion channels) interaction network</i> | | | | | | | | |
| Global | 0.85 | 0.79 | 0.31 | 0.21 | 0.97 | 0.93 | 0.78 | 0.73 |
| Loc. so | 0.81 | 0.80 | 0.33 | 0.23 | 0.97 | 0.93 | 0.78 | 0.74 |
| Loc. mo | - | 0.79 | 0.33 | 0.22 | - | 0.93 | 0.79 | 0.74 |
| <i>Drug-protein (GPCR) interaction network</i> | | | | | | | | |
| Global | 0.67 | 0.53 | 0.32 | 0.16 | 0.95 | 0.85 | 0.86 | 0.81 |
| Local so | 0.60 | 0.53 | 0.33 | 0.18 | 0.95 | 0.84 | 0.85 | 0.80 |
| Local mo | - | 0.51 | 0.31 | 0.16 | - | 0.84 | 0.85 | 0.81 |
| <i>Drug-protein (nuclear receptors) interaction network</i> | | | | | | | | |
| Global | 0.45 | 0.29 | 0.35 | 0.13 | 0.84 | 0.60 | 0.79 | 0.66 |
| Local so | 0.43 | 0.27 | 0.36 | 0.12 | 0.86 | 0.59 | 0.80 | 0.65 |
| Local mo | - | 0.27 | 0.35 | 0.12 | - | 0.59 | 0.80 | 0.66 |

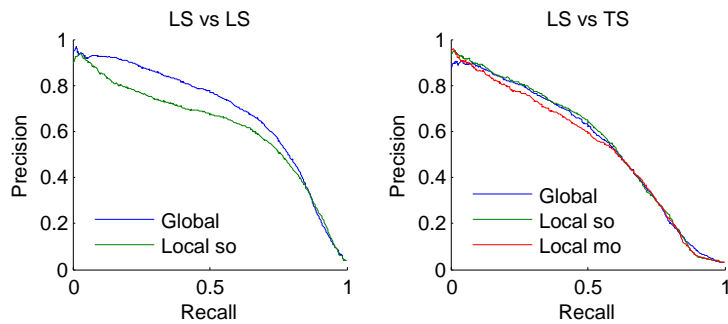
Drug-protein (enzymes) interaction network:

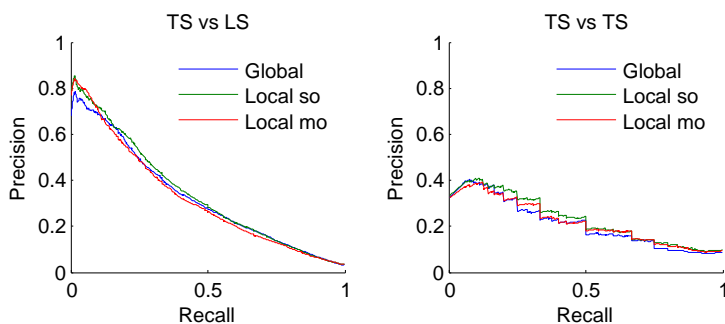


Drug-protein (ion channels) interaction network:

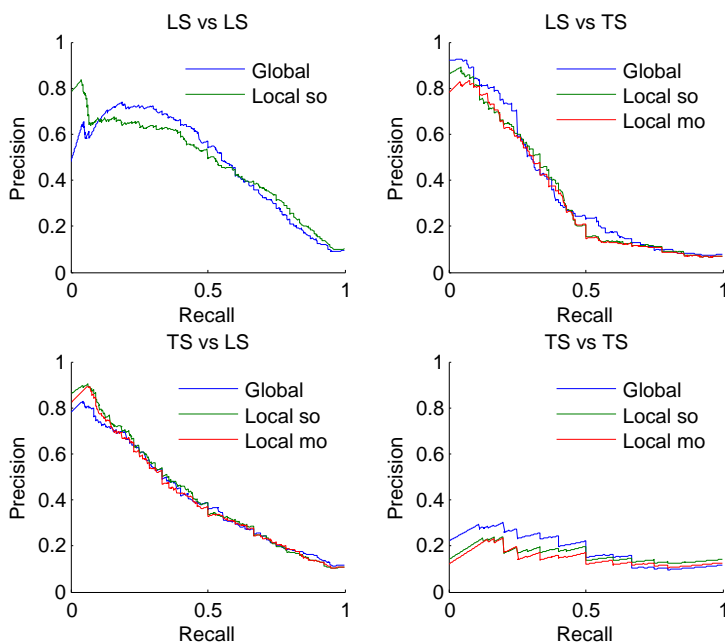


Drug-protein (GPCR) interaction network:





Drug-protein (nuclear receptors) interaction network:



Comparison with literature. [43] and [3] use SVM to predict the four classes of drug-protein interaction network. The first one used a kernel regression-based method (KRM): a global approach in which they integrated the chemical and genomic spaces into a unified space. The second one used bipartite local models (BLM) and then did not predict $TS \times TS$ interactions. We compared the AUPR of these two methods with ours, in a 10 times 10-fold CV, in the following Table. Extra-Trees (E-T) is comparable to the other methods, sometimes giving better results (for DPI-I) and sometimes giving less good results (for DPI-N).

[10] developed three different supervised inference methods, which they tested on the four DPI datasets. The methods are drug-based similarity inference (DBSI), target-based similarity inference (TBSI) and network-based inference (NBI). The last one only use network topology similarity to to infer new targets for known drugs. NBI gives the best performance of the three but has the disadvantage to only be able to predict $LS \times LS$ pairs. Extra-Trees give better or equal results than these three methods, when doing 10 times 10-fold CV. Results are presented in the following Table.

| | Method | Precision-Recall | | | Method | ROC |
|--------------|------------------|------------------|-------|-------|-------------------|-------|
| | | LS-LS | LS-TS | TS-LS | | LS-LS |
| <i>DPI-E</i> | KRM ¹ | 0.83 | 0.81 | 0.38 | DBSI ³ | 0.78 |
| | BLM ² | 0.83 | 0.81 | 0.39 | TBSI ³ | 0.90 |
| | E-T | 0.87 | 0.79 | 0.32 | NBI ³ | 0.97 |
| <i>DPI-I</i> | KRM | 0.76 | 0.81 | 0.31 | DBSI | 0.71 |
| | BLM | 0.77 | 0.80 | 0.32 | TBSI | 0.90 |
| | E-T | 0.85 | 0.80 | 0.34 | NBI | 0.98 |
| <i>DPI-G</i> | KRM | 0.67 | 0.62 | 0.41 | DBSI | 0.76 |
| | BLM | 0.65 | 0.55 | 0.38 | TBSI | 0.75 |
| | E-T | 0.68 | 0.55 | 0.34 | NBI | 0.94 |
| <i>DPI-N</i> | KRM | 0.74 | 0.61 | 0.51 | DBSI | 0.79 |
| | BLM | 0.58 | 0.35 | 0.40 | TBSI | 0.53 |
| | E-T | 0.48 | 0.36 | 0.42 | NBI | 0.84 |

¹ [43]

² [3]

³ [10]

References

- [1] Asa Ben-Hur and William Stafford Noble. Kernel methods for predicting protein-protein interactions. *Bioinformatics*, 21:i38–i46, 2005.
- [2] Kevin Bleakley, Gerard Biau, and Jean-Philippe Vert. Supervised reconstruction of biological networks with local models. *Bioinformatics*, 23:i57–i65, 2007.
- [3] Kevin Bleakley and Yoshihiro Yamanishi. Supervised prediction of drug-target interactions using bipartite local models. *Bioinformatics*, 25(18):2397–2403, 2009.
- [4] H. Blockeel, L. De Raedt, and J. Ramon. Top-down induction of clustering trees. In *Proceedings of ICML 1998*, pages 55–63, 1998.
- [5] L. Breiman, J.H. Friedman, R.A. Olsen, and C.J. Stone. *Classification and Regression Trees*. Wadsworth International, 1984.
- [6] Leo Breiman. Random forests. *Machine learning*, 45(1):5–32, 2001.
- [7] Sylvain Brohée, Rekin’s Janky, Fadi Abdel-Sater, Gilles Vanderstocken, Bruno André, and Jacques van Helden. Unraveling networks of co-regulated genes on the sole basis of genome sequences. *Nucleic Acids Res.*, 39(15):6340–6358, 2011.
- [8] Céline Brouard, Florence D’Alche-Buc, and Marie Szafranski. Semi-supervised penalized output kernel regression for link prediction. In Lise Getoor and Tobias Scheffer, editors, *Proceedings of the 28th International Conference on Machine Learning (ICML-11)*, ICML ’11, pages 593–600, New York, NY, USA, June 2011. ACM.

- [9] Xue-Wen Chen and Mei Liu. Prediction of protein-protein interactions using random decision forest framework. *Bioinformatics*, 21:4394–4400, 2005.
- [10] Feixiong Cheng, Chuang Liu, Jing Jiang, Weiqiang Lu, Weihua Li, Guixia Liu, Weixing Zhou, Jin Huang, and Yun Tang. Prediction of drug-target interactions and drug repositioning via network-based inference. *PLoS Computational Biology*, 8(5), 2012.
- [11] Gordon Chua, Quaid D. Morris, Richelle Sopko, Mark D. Robinson, Owen Ryan, Esther T. Chan, Brendan J. Frey, Brenda J. Andrews, Charles Boone, , and Timothy R. Hughes. Identifying transcription factor functions and targets by phenotypic activation. *PNAS*, 103:12045–12050, 2006.
- [12] Jesse Davis and Mark Goadrich. The relationship between precision-recall and roc curves. *Proceedings of the 23rd International Conference on Machine Learning*, 2006.
- [13] F Denis, R Gilleron, and F Letouzey. Learning from positive and unlabeled examples. *Theoretical Computer Science*, 348(1):70–83, 2005.
- [14] C Elkan and K Noto. Learning classifiers from only positive and unlabeled data. In *KDD '08 Proceeding of the 14th ACM SIGKDD international conference on Knowledge discovery and data mining*, pages 213–220, 2008.
- [15] Jeremiah J Faith, Boris Hayete, Joshua T Thaden, Ilaria Mogno, Jamey Wierzbowski, Guillaume Cottarel, Simon Kasif, James J Collins, and Timothy S Gardner. Large-scale mapping and validation of escherichia coli transcriptional regulation from a compendium of expression profiles. *PLoS Biol*, 5(1):e8, 2007.
- [16] JJ Faith, ME Driscoll, VA Fusaro, EJ Cosgrove, B Hayete, FS Juhn, SJ Schneider, and TS Gardner. Many microbe microarrays database: uniformly normalized affymetrix compendia with structured experimental metadata. *Nucleic Acids Research*, 36:866–870, 2007.
- [17] P. Geurts, D. Ernst, and L. Wehenkel. Extremely randomized trees. *Machine Learning*, 63(1):3–42, 2006.
- [18] Pierre Geurts, Alexandre Irrthum, and Louis Wehenkel. Supervised learning with decision tree-based methods in computational and systems biology. *Molecular BioSystems*, 5:1593–1605, dec 2009.
- [19] Pierre Geurts, Nizar Touleimat, Marie Dutreix, and Florence d’Alché Buc. Inferring biological networks with output kernel trees. *BMC Bioinformatics*, 8(Suppl 2):S4, 2007.
- [20] Jesse Gillis and Paul Pavlidis. The impact of multifunctional genes on ”guilt by association” analysis. *PLoS ONE*, 6(2), 2011.
- [21] Maureen Hillenmeyer et al. The chemical genomic portrait of yeast: Uncovering a phenotype for all genes. *Science*, 320:362–365, 2008.
- [22] Zhanzhi Hu, Patrick J Killion, and Vishwanath R Iyer. Genetic reconstruction of a functional transcriptional regulatory network. *Nature genetics*, 39:683–687, 2007.
- [23] Martial Hue and Jean-Philippe Vert. On learning with kernels for unordered pairs. In *Proceedings of the 27th International Conference on Machine Learning*, Haifa, Israel, 2010.
- [24] TR Hughes, MJ Marton, AR Jones, CJ Roberts, R Stoughton, CD Armour, HA Bennett, E Coffey, H Dai, YD He, MJ Kidd, AM King, MR Meyer, D Slade, PY Lum, SB Stepaniants, DD Shoemaker, D Gachotte, K Chakraborty, J Simon, M Bard, and SH Friend. Functional discovery via a compendium of expression profiles. *Cell*, 102:109–126, 2000.

- [25] T. Kato, K. Tsuda, and A. Kiyoshi. Selective integration of multiple biological data for supervised network inference. *Bioinformatics*, 21(10):2488–2495, 2005.
- [26] Nan Lin, Baolin Wu, Ronald Jansen, Mark Gerstein, and Hongyu Zhao. Information assessment on predicting protein-protein interactions. *BMC Bioinformatics*, 5:154, 2004.
- [27] Kenzie D MacIsaac, Ting Wang, Benjamin Gordon, David K Gifford, Gary D Stormo, and Ernest Fraenkel. An improved map of conserved regulatory sites for *saccharomyces cerevisiae*. *BMC Bioinformatics*, March 2006.
- [28] Sara Madeira and Arlindo Oliveira. Biclustering Algorithms for Biological Data Analysis: A Survey. *IEEE/ACM Transactions on Computational Biology and Bioinformatics (TCBB)*, 1(1), 2004.
- [29] Christian Von Mering, Roland Krause, Berend Snel, Michael Cornell, Stephen G. Oliver, Stanley Fields, and Peer Bork. Comparative assessment of large-scale data sets of protein-protein interactions. *Nature*, 417:399–403, 2002.
- [30] Fantine Mordelet and Jean-Philippe Vert. Sirene: supervised inference of regulatory networks. *Bioinformatics*, 24(16):i76–i82, 2008.
- [31] Y. Qi, J. Klein-seetharaman, Z. Bar-joseph, Yanjun Qi, and Ziv Bar-joseph. Random forest similarity for protein-protein interaction prediction. *Pac Symp Biocomput*, 2005:531–542, 2005.
- [32] Yanjun Qi, Ziv Bar-Joseph, and Judith Klein-Seetharaman. Evaluation of different biological data and computational classification methods for use in protein interaction prediction. *Proteins*, 63(3):490–500, 2006.
- [33] Marie Schrynemackers, Robert Kuffner, and Pierre Geurts. On protocols and measures for the validation of supervised methods for the inference of biological networks. *Frontiers in Genetics*, 4(262), 2013.
- [34] Maya Schuldiner, SR Collins, NJ Thompson, V Denic, A Bhamidipati, T Punna, J Ihmels, B Andrews, C Boone, JF Greenblatt, JS Weissman, and NJ Krogan. Exploration of the function and organization of the yeast early secretory pathway through an epistatic miniarray profile. *Cell*, 123:507–519, 2005.
- [35] Y. Tabei, E. Pauwels, V. Stoven, K. Takemoto, and Y. Yamanishi. Identification of chemogenomic features from drug-target interaction networks using interpretable classifiers. *Bioinformatics*, 28:i487–i494, 2012.
- [36] Oznur Tastan, Yanjun Qi, Jaime G. Carbonell, and Judith Klein-Seetharaman. Prediction of interactions between hiv-1 and human proteins by information integration. *Pacific Symposium on Biocomputing*, 14:516–527, 2009.
- [37] Grigorios Tsoumakas and Ioannis Katakis. Multi-label classification: An overview. *International Journal of Data Warehousing and Mining (IJDWM)*, 3(3):1–13, 2007.
- [38] Jean-Philippe Vert. Reconstruction of biological networks by supervised machine learning approaches. In *Elements of Computational Systems Biology*, chapter 7, pages 165–188. John Wiley & Sons, Inc., 2010.
- [39] Jean-Philippe Vert, Jian Qiu, and William S Noble. A new pairwise kernel for biological network inference with support vector machines. *BMC Bioinformatics*, 8(Suppl 10):S8, 2007.

- [40] Y. Yamanishi, E. Pauwels, H. Saigo, and V. Stoven. Extracting sets of chemical substructures and protein domains governing drug-target interactions. *Journal of Chemical Information and Modeling*, page 110505071700060, May 2011.
- [41] Y. Yamanishi and J.-P. Vert. Protein network inference from multiple genomic data: a supervised approach. *Bioinformatics*, 20:i363–i370, 2004.
- [42] Y. Yamanishi and J.-P. Vert. Supervised enzyme network inference from the integration of genomic data and chemical information. *Bioinformatics*, 21:i468–i477, 2005.
- [43] Yoshihiro Yamanishi, Michihiro Araki, Alex Gutteridge, Wataru Honda, and Minoru Kanehisa. Prediction of drug-target interaction networks from the integration of chemical and genomic spaces. *Bioinformatics*, 24(13):i232–i240, 2008.
- [44] Hua Yu, Jianxin Chen, Xue Xu, Yan Li, Huihui Zhao, Yupeng Fang, Xiuxiu Li, Wei Zhou, Wei Wang, and Yonghua Wang. A systematic prediction of multiple drug-target interactions from chemical, genomic, and pharmacological data. *PLoS ONE*, 7(5), 2012.